NeuroImage 64 (2013) 601–615

Contents lists available at SciVerse ScienceDirect

NeuroImage

journal homepage: www.elsevier.com/locate/ynimg

Disentangling common and specific neural subprocesses of response inhibition

A. Sebastian [a,b,h,*], M.F. Pohl [a,b], S. Klöppel [a,b], B. Feige [a,b], T. Lange [b,e], C. Stahl [f], A. Voss [g], K.C. Klauer [d], K. Lieb [h], O. Tüscher [a,b,c,h]

[a] Albert-Ludwigs-University Freiburg, Department of Psychiatry and Psychotherapy, Germany
[b] Albert-Ludwigs-University Freiburg, Division Freiburg Brain Imaging, Germany
[c] Albert-Ludwigs-University Freiburg, Department of Neurology, Germany
[d] Albert-Ludwigs-University Freiburg, Department of Psychology, Germany
[e] Albert-Ludwigs-University Freiburg, Department of Radiology, Germany
[f] University of Cologne, Department of Psychology, Germany
[g] Ruprecht-Karls-University Heidelberg, Department of Psychology, Germany
[h] Johannes-Gutenberg-University Mainz, Department of Psychiatry and Psychotherapy, Germany

ARTICLE INFO

Article history:
Accepted 4 September 2012
Available online 14 September 2012

Keywords:
Impulse control
Simon task
Go/no-go task
Stop-signal task
Inferior frontal gyrus
Pre-supplementary motor area

ABSTRACT

Response inhibition is disturbed in several disorders sharing impulse control deficits as a core symptom. Since response inhibition is a cognitively and neurally multifaceted function which has been shown to rely on differing neural subprocesses and neurotransmitter systems, further differentiation to define neurophysiological endophenotypes is essential. Response inhibition may involve at least three separable cognitive subcomponents, i.e. interference inhibition, action withholding, and action cancelation. Here, we introduce a novel paradigm – the Hybrid Response Inhibition task – to disentangle interference inhibition, action withholding and action cancelation and their neural subprocesses within one task setting during functional magnetic resonance imaging (fMRI). To validate the novel task, results were compared to a battery of separate, standard response inhibition tasks independently capturing these subcomponents and subprocesses. Across all subcomponents, mutual activation was present in the right inferior frontal cortex (rIFC), pre-supplementary motor area (pre-SMA) and parietal regions. Interference inhibition revealed stronger activation in pre-motor and parietal regions. Action cancelation resulted in stronger activation in fronto-striatal regions. Our results show that all subcomponents share a common neural network and thus all constitute different subprocesses of response inhibition. Subprocesses, however, differ to the degree of regional involvement: interference inhibition relies more pronouncedly on a fronto-parietal–pre-motor network suggesting its close relation to response selection processes. Action cancelation, in turn, is more strongly associated with the fronto-striatal pathway implicating it as a late subcomponent of response inhibition. The new paradigm reliably captures three putatively subsequent subprocesses of response inhibition and might be a promising tool to differentially assess disturbed neural networks in disorders showing impulse control deficits.

Introduction

Response inhibition is the ability to suppress inadequate but inadvertently activated, prepotent or ongoing response tendencies (Barkley, 1997; Miyake et al., 2000; Nigg, 2000). In terms of reactive control, response inhibition addresses inhibition in response to external stimuli (for a review see Aron, 2011). Such inhibitory control is ubiquitous in our daily routines like stopping at a traffic light turning red despite being in a hurry. Therefore, it is fundamental to individual and social functioning (Evenden, 1999).

Recently, the need to precisely specify different components and underlying neural substrates of impulse control specifically response inhibition has been increasingly demanded (Aron, 2011; Dalley et al., 2011; Eagle et al., 2008; Nee et al., 2007; Schachar et al., 2007; Swick et al., 2011). Even if different tasks that tap into subprocesses of response inhibition may share common features, inhibition might be required at different time points in the programming and generation of the response output and rely on different neural substrates (Dalley et al., 2011; Nee et al., 2007; Schachar et al., 2007; Swick et al., 2011). At the same time, apparently closely related response inhibition tasks, e.g. Go/no-go- and the Stop-signal tasks, were shown to be modulated by different transmitter systems (Eagle et al. 2008) and, thereby, neurocognitively dissociable. A more precise delineation of common and specific neural subprocesses of response inhibition and related paradigms to capture such subprocesses thus is inevitable to provide a coherent framework to possibly identify disease-related endophenotypes.

* Corresponding author at: Johannes-Gutenberg-University Mainz, Department of Psychiatry and Psychotherapy, Untere Zahlbacher Str. 8, 55131 Mainz, Germany. Fax: +49 6131 17 6690.
E-mail addresses: alexandra.sebastian@uniklinik-freiburg.de, alexandra.sebastian@unimedizin-mainz.de (A. Sebastian).

1053-8119/$ – see front matter © 2012 Elsevier Inc. All rights reserved.
http://dx.doi.org/10.1016/j.neuroimage.2012.09.020

A variety of paradigms have been employed to study response inhibition such as Stop-signal-, Go/no-go-, Continuous Performance-, Simon-, Antisaccade-, or Flanker-tasks, all requiring inhibitory control over prepotent response tendencies (Aron, 2011; Nee et al., 2007). Using functional magnetic resonance imaging (fMRI) during such tasks, several neural key regions associated with inhibitory processes have been revealed, especially the right inferior frontal cortex (rIFC), pre-supplementary motor area (pre-SMA), basal ganglia and subthalamic nucleus (STN) (e.g. Aron, 2011; Boehler et al., 2010; Chikazoe, 2010; Jahfari et al., 2011; Levy and Wagner, 2011; Swick et al., 2011).

Although inhibition in the above mentioned tasks is associated with largely overlapping activation patterns, recent research suggests that these patterns are not identical. A recent meta-analysis by Swick et al. (2011) revealed common activation in Go/no-go- and Stop-signal tasks mainly in the right anterior insula and the pre-supplemental motor area (pre-SMA). Inhibition in Stop-signal tasks was, however, more strongly associated with activation in the left anterior insula and the thalamus, while inhibition in Go/no-go tasks relied more on activation in the right middle frontal gyrus (MFG) and parietal regions. Studies employing separate Go/no-go- and Stop-signal tasks in the same subjects revealed common activation in bilateral IFC (McNab et al., 2008; Rubia et al., 2001), right MFG (McNab et al., 2008; Rubia et al., 2001; Zheng et al., 2008), pre-SMA and inferior parietal lobe (Rubia et al., 2001). Activation in the Go/no-go task compared to the Stop-signal task was more pronounced in the left MFG, pre-SMA, and inferior parietal regions while no increased activation was present during Stop-signal tasks (Rubia et al., 2001). Thus, findings regarding common and distinct neural correlates during Go/no-go- and Stop-signal tasks remain divergent.

Behavioral and imaging evidence suggests that inhibition during Simon- and Stop-signal tasks relies on similar mechanisms with common neural correlates (Nee et al., 2007; Verbruggen et al., 2005). Comparing inhibition in the Simon task, which involves a stimulus–response conflict, to tasks involving a stimulus–stimulus conflict (e.g. Stroop task) revealed increased activation mainly in pre-motor, thus more response related regions (Egner et al., 2007; Liu et al., 2004; Wendelken et al., 2009). Other studies have linked parietal activation to both, stimulus–response conflict (Frühholz et al., 2011; Wendelken et al., 2009) and to stimulus–stimulus conflict (Egner et al., 2007; Liu et al., 2004).

Taken together, recent research increasingly suggests that distinguishable components of response inhibition exist, which may be tapped by employing different paradigms (Band and van Boxtel, 1999; Dalley et al., 2011; Eagle et al., 2008; Nee et al., 2007; Schachar et al., 2007; Swick et al., 2011; Verbruggen and Logan, 2008). However, this has yet not been shown in direct comparison of three components within one paradigm. Thus, component-specific neural correlates remain largely unclear. To address this question and thereby meeting the increasing demand for a more precise delineation of mutual and specific neural subprocesses of response inhibition, we introduce a novel task, the Hybrid Response Inhibition (HRI) task, comprising features of Simon-, Go/no-go- and Stop-signal tasks. The Simon task is thought to involve a conflict of response selection by involuntarily co-activating response tendencies due to incongruent stimulus dimensions ('interference inhibition'; Simon and Berbaum, 1990). The ability to withhold a motor response ('action withholding'; cf. Schachar et al., 2007) is usually assessed using a Go/no-go task in which rare no-go-stimuli instead of frequent go-stimuli are presented requiring inhibition of a prepotent response tendency. In a Stop-signal task, in contrast, rare stop-signals occur at some delay after the go stimuli, thus requiring an inhibition of an already ongoing motor response ('action cancelation'; cf. Schachar et al., 2007). By using identical visual stimulus material across conditions within one task, we compare conditions designed to distinguish between different subcomponents of response inhibition, enabling us to study functional and spatial segregation and specialization of underlying neural subprocesses of response inhibition. To assess the validity of the novel task, we additionally assessed interference inhibition, action withholding and action cancelation in separate, commonly employed versions of the Simon-, Go/no-go- and Stop-signal tasks in another sample of participants.

We hypothesized that the subcomponents of response inhibition, i.e. interference inhibition, action withholding and action cancelation share common neural pathways of response inhibition which should be observable as mutual activation in the same key regions of the neural inhibitory network. However, these subcomponents should differ in the extent to which they recruit individual regions of the neural inhibitory network. We further hypothesized based on previous findings that interference inhibition is associated more strongly with activation in pre-motor and parietal regions, action withholding with middle frontal gyrus and parietal regions, whereas action cancelation relies more strongly on bilateral prefrontal and striatal activation.

Materials and methods

Participants

Twenty-one healthy subjects were assessed using the novel task (12 males, mean age = 24.24 ± 2.3 years). Twenty-four healthy subjects were assessed using the battery of three separate standard tasks (9 males, mean age = 27.42 ± 5.6 years). All subjects were right handed as determined by the Edinburgh Handedness Inventory (Oldfield, 1971) and had normal or corrected to normal vision. Subjects had no lifetime history of axis I or axis II disorders as thoroughly assessed by a trained psychologist using the Structured Clinical Interview for DSM-IV Axis I and II disorders (Wittchen et al., 1997). All subjects were screened for factors contradicting MRI scanning, provided written informed consent and were compensated for their time. The study was approved by the Ethics Committee of the University of Freiburg Medical School.

Tasks

Hybrid Response Inhibition Task (HRI)

The HRI task is a newly developed paradigm incorporating the properties of the Simon-, the Go/no-go-, and the Stop-signal tasks. Using identical stimulus material we can, thus, capture the subcomponents of response inhibition interference inhibition, action withholding and action cancelation within one paradigm. This allows for a direct contrast of the subcomponents to test for component specific functional segregation within the inhibitory network within one task setting.

Subjects performed three runs of the HRI task during the scanning session (Fig. 1). The task was programmed in Presentation software (version 13.0, www.neurobs.com). Before the scanning session, all subjects received a brief training session on a laptop computer. Prior to the beginning of each run, instructions were given orally and subjects were reminded to respond as quickly and as accurately as possible. Each run was preceded by a visual presentation of the instruction for 5000 ms followed by a rest period of 5000 ms during which a fixation cross was presented in the center of the screen. At the end of each run, a fixation cross was again presented for the same duration. Throughout the scanning session, subjects were asked to hold a MR compatible response button box in each hand and to respond to the stimuli by pressing the response button with the left or right index finger.

The task consisted of four conditions: a congruent go condition (62.5%), an incongruent go condition (12.5%), a no-go condition (12.5%) and a stop condition (12.5%). Subjects were asked to fixate a white cross at all times, which was presented in the center of the screen against a black background. Each trial started with a white ellipse encircling the cross. After 500 ms, a white arrow appeared within the ellipse either on the right or left side of the fixation cross for 1000 ms or until a button press was performed. Subjects were instructed to respond corresponding to the pointing direction of the arrows (left index finger button press for an arrow pointing to the left and a right index finger button press for an arrow pointing to the right) and to attempt to withhold the reaction in

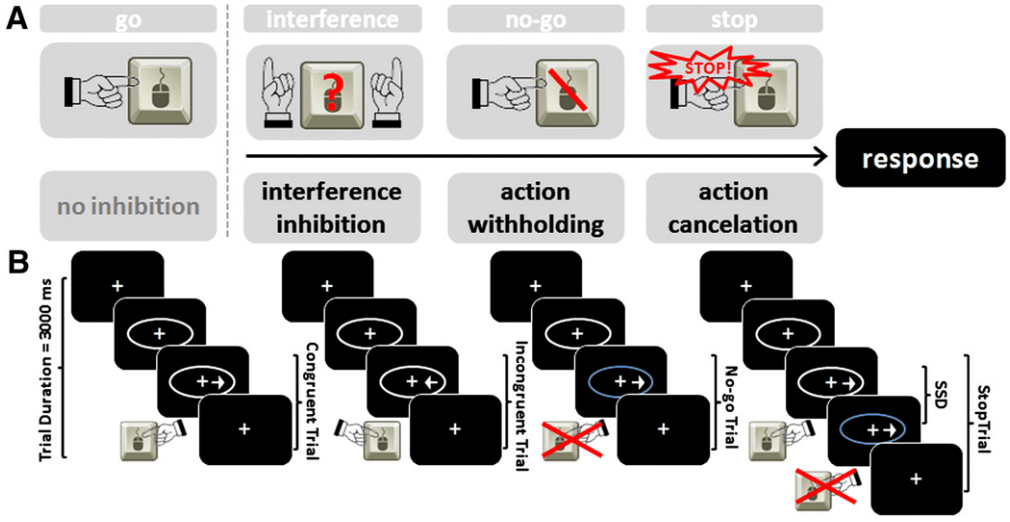

Fig. 1. Schematic representation of the subcomponents of response inhibition (A), and associated trial type in the Hybrid Response Inhibition task (B). Subjects were instructed to press a button corresponding to the pointing direction of an arrow. Go trials consisted of congruent trials; inhibition trials consisted of incongruent trials (interference inhibition), occurrence of a no-go stimulus (blue ellipse; action withholding), or of a stop-signal (blue ellipse after a varying stop-signal delay (SSD); action cancelation).

case of the ellipse turning blue. Instructions equally stressed speed and accuracy of responding.

In the congruent go condition a right pointing arrow was presented in the right half of the ellipse, or a left pointing arrow was presented in the left half of the ellipse. In the incongruent go condition a right pointing arrow was presented in the left half of the screen, or a left pointing arrow was presented in the right half of the screen. In the no-go condition (which was always a congruent condition) the ellipse changed its color from white to blue at the onset of the arrow. In the stop condition (which was also always a congruent condition) the ellipse changed its color from white to blue after a variable stop-signal delay (SSD) following the onset of the arrow. The SSD was adapted to the participants' performance following a staircase procedure to yield a probability of 50% of correct inhibitions per run. In the beginning of a run the SSD was 220 ms. If the response was not inhibited (commission error) the SSD was decreased by 50 ms with a minimum SSD of 20 ms and the blue circle and the arrow remained on the screen. If a response was inhibited (correct stop) the SSD was increased by 50 ms and the circle and the arrow disappeared.

The length of the interstimulus interval was jittered with a mean duration of 1500 ms and a standard deviation of 372 ms. A run consisted of 160 trials that were presented in a pseudo-randomized order.

Separate response inhibition tasks

Another sample of participants performed three separate tasks within one scanning session, a Simon-, Go/no-go-, and Stop-signal task, with each task consisting of two consecutive runs. The order of the tasks was counterbalanced across subjects. Tasks and experimental procedures were identical to those described before (Sebastian et al., 2012) and are briefly explained here and in Fig. 2. These tasks were deliberately designed to maximize comparability with previous studies (Aron and Poldrack, 2006; Garavan et al., 1999; Kerns, 2006).

Simon task. A white cross was presented in the center of the screen against a black background which subjects were asked to fixate at all times. Either on the left or the right half of the screen, a white arrow was presented for 1000 ms or until a button press was performed. Subjects were instructed to respond corresponding to the pointing direction of the arrows. In the congruent condition, a right pointing arrow was presented in the right half of the screen, or a left pointing arrow was presented in the left half of the screen. In the incongruent condition, a right pointing arrow was presented in the left half of the screen, or a left pointing arrow was presented in the right half of the screen. Stimuli were presented in randomized order. The length of the interstimulus interval was jittered with a mean duration of 2723 ms and a standard deviation of 422 ms. Per run, 100 stimuli were displayed with 50% being congruent and 50% being incongruent trials.

Go/no-go task. A stream of consonants was presented serially in the center of the screen. Every stimulus was displayed for 500 ms immediately followed by a blank screen for 500 ms. Subjects were instructed to make a right index finger button press for every letter (go stimulus) except for the letter "X" (no-go stimulus). For the go stimuli, a letter was randomly chosen from all consonants of the alphabet except the "X". Mean probability for no-go stimuli was 29% and a no-go stimulus was always followed by a go stimulus. Per run, 300 stimuli were presented.

Stop-signal task. The Stop-signal task consisted of a go condition and a stop condition. Each trial started with a white fixation ring which was presented in the center of the screen. After 500 ms, a white arrow appeared within the fixation ring. The arrow and the fixation ring were presented for a maximum of 1000 ms or until a button press was performed. Subjects were instructed to respond with a button press corresponding to the pointing direction of the arrows. In the stop condition, which occurred in 25% of the trials, a stop-signal was presented after a variable SSD. The stop-signal consisted of a change in color of the fixation ring from white to blue. Subjects were instructed to attempt to cancel the reaction in case of a stop-signal. The SSD was adapted to the participants' performance following a staircase procedure to yield a probability of 50% of correct inhibitions per run. In the beginning of a run, the SSD was 220 ms. If the response was not inhibited, the arrow disappeared and the SSD was decreased by 50 ms in the next stop trial with a minimum SSD of 70 ms. If a response was inhibited correctly, the blue circle and the arrow remained on the screen and the SSD was increased by 50 ms in the next stop trial. The length of the interstimulus interval was jittered with a mean duration of 1000 ms and a standard deviation of 292 ms. A run consisted of 128 stimuli, which were presented in a pseudo-randomized order.

MRI data acquisition

Images were acquired on a Magnetom Trio 3 T system (Siemens, Germany), equipped with a 12-channel head coil for signal reception. Stimuli were projected on a screen at the head end of the scanner bore and were viewed with the aid of a mirror mounted on the head

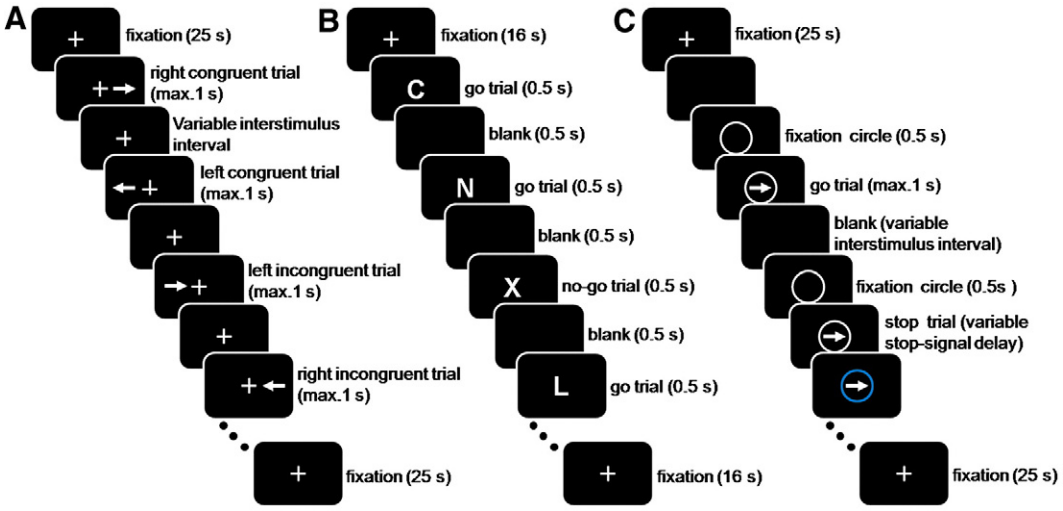

Fig. 2. Schematic display of (A) Simon task, (B) Go/no-go task and (C) Stop-signal task. Subjects were instructed to press a button corresponding to the pointing direction of an arrow (Simon task and Stop-signal task) or for any letter except the "X" (Go/no-go task). Inhibition trials consisted of incongruent trials in the Simon task, occurrence of a no-go stimulus in the Go/no-go task or of a stop signal in the Stop-signal task.

coil. Foam padding was used to limit head motion within the coil. Functional T2*-weighted echo-planar imaging (EPI) was performed (TR = 2250 ms, TE = 30 ms, flip angle = 90°, FOV = 192 mm, voxel size = $3 \times 3 \times 3$ mm^3, 36 slices) applying fully automated PACE motion correction (Thesen et al., 2000) and distortion correction based on point spread function mapping (Zaitsev et al., 2004). For the HRI task, 230 whole brain volumes were acquired per run resulting in a total duration of 517.5 s. For the Simon task, 153 whole brain volumes were acquired per run resulting in a total duration of 344.25 s; for the Go/no-go task, 157 whole brain volumes were acquired per run resulting in a total duration of 353.25 s; as the Stop-signal task was adaptive to reaction time, an average of 150 whole brain volumes were acquired per run resulting in a mean duration of 337.5 s. Following the functional protocol, a high resolution T1-weighted anatomical data set was obtained using an 3D magnetization prepared rapid acquisition gradient echo (MPRAGE) sequence for registration purposes (TR = 2200 ms, TE = 4.11 ms, flip angle = 12°, FOV = 256 mm, voxel size $1 \times 1 \times 1$ mm^3).

MRI data analysis

Image preprocessing

SPM 8 (Wellcome Department of Cognitive Neurology) was used to conduct all image preprocessing and statistical analyses, running with Matlab 7.9 (The Mathworks Inc., Natick, Massachusetts, USA). Images were screened for motion artifacts prior to data analysis. No excessive head motion (>2 mm) was observed in any of the subjects. Next, images were reoriented to the T1-template of SPM. The first five functional images of each run were discarded to allow for equilibrium effects. Then, several preprocessing steps were carried out on the remaining functional images for each task separately. To spatially correct for residual inter-scan movement artifacts, images were realigned to the first image of the first run, using a six degrees-of-freedom rigid body transformation. The realigned functional images were co-registered to the individual anatomical T1 image. Subsequently, the anatomical image was spatially normalized (linear and nonlinear transformations) into the reference system of the Montreal Neurological Institute's (MNI) reference brain using standard templates and normalization parameters were applied to all functional images. Finally, the normalized functional data were smoothed with a three-dimensional isotropic Gaussian kernel (8 mm full-width at half maximum, FWHM) to enhance signal-to-noise ratio and to allow for residual differences in functional neuroanatomy between subjects.

Single subject analysis

A linear regression model (general linear model, GLM) was fitted to the fMRI data from all subjects. Significant hemodynamic changes for each condition were assessed using *t*-statistics. All events were modeled as stick functions at stimulus onset and convoluted with a canonical hemodynamic response function. The model included a high-pass filter with a cut-off period of 128 s to remove drifts or other low-frequency artifacts in the time series.

HRI-task. After convolution with a canonical hemodynamic response function four event types were modeled as regressors of interest: correct reactions for congruent go, incongruent go, no-go and stop trials. Additionally, incorrect reactions for each condition and instruction and fixation cross were modeled as regressors of no interest.

Separate tasks. For the Simon task, four event types were modeled: correct and incorrect reactions for congruent and incongruent trials, respectively. The few incongruent trials preceded by an identical condition (e.g. a right pointing arrow was presented on the left side in two subsequent trials) were modeled separately. These trials were not included in the second level analysis based on the assumption that less inhibition will be necessary in subsequent incongruent trials. For comparison with the other tasks, correct incongruent and correct congruent trials will later be referred to as Simon successful inhibition and Simon go trials, respectively.

For the Go/no-go task, correct and incorrect no-go events were modeled as regressors of interest. Frequent go-stimuli were used as an active baseline to allow for an inhibition-specific contrast of 'correct inhibition minus go' despite the short inter-stimulus interval.

For the Stop-signal task, five events were modeled: correct and incorrect reactions as well as omissions in the go condition and correct and incorrect reactions in the stop condition (successful inhibition and commission errors, respectively). For each task, instruction and fixation cross were modeled as regressors of no interest.

Group analysis

Task validation. First, we conducted random effects second level analyses (one-sample *t*-tests) to identify predictive voxels across subjects separately for each subcomponent of response inhibition to validate that the HRI task reliably captures the subcomponents of response inhibition and the corresponding neural subprocesses. In the HRI task as well as in the three separate tasks, the corresponding contrasts of

Table 1
Behavioral results.

	HRI task	Simon task	Go/no-go task	Stop-signal task	F (1,43)
RT (go) [ms]	528.08 ± 113.82	479.20 ± 57.47	397.10 ± 60.54***	490.14 ± 94.29	24.06
No-go/stop commissions [%]	3.17 ± 4.59/ 45.79 ± 11.10	n.a.	10.86 ± 7.46***	47.12 ± 6.55	16.72
Interference effect [ms]	69.14 ± 42.13	58.19 ± (33.64)	n.a.	n.a.	0.94
SSRT [ms]	288.49 ± 45.79	n.a.	n.a.	259.84 ± 40.50**	12.35

Mean reaction time (RT) of go trials, interference effect and Stop-signal reaction time (SSRT) in milliseconds, mean % of commission errors of no-go/stop trials, and standard deviation (SD). Percentage error is estimated by dividing the number of incorrect no-go/stop trials by the total number of the trial type. Interference effect is calculated by subtracting the mean RT of congruent trials from the mean RT of incongruent trials. SSRT is calculated by subtracting the mean stop-signal delay from the median RT (go). ** = p<0.01; *** p<0.001; n.a. = not applicable.

'successful inhibition — go' were calculated. For each HRI component, independent one-sample *t*-tests were computed for the following contrasts: (i) interference inhibition: incongruent go — congruent go; (ii) action withholding: no-go — congruent go; (iii) action cancelation: stop — congruent go. For the separate tasks, independent one-sample *t*-tests were computed for the corresponding contrasts: (i) Simon task: incongruent — congruent; (ii) Go/no-go task: no-go — go (active baseline); (iii) Stop-signal task: stop — go.

To explicitly assess the validity of the novel HRI task relative to the established single tasks, a sequential masking approach was used following Klöppel et al. (2007). This procedure allows exploring common activation in different tasks despite differing stimulus material. The statistical images containing the *t*-values (*t*-maps) obtained in a one-sample *t*-tests of one of the separate tasks were used to define a region of interest for the *t*-map obtained in the corresponding *t*-test of the HRI task. *T*-maps used for mask generation were thresholded at $p<0.05$ (uncorrected). For instance, the *t*-map containing voxels associated with successful inhibition in the Stop-signal task (successful stop — go) were used to generate an inclusive mask for the *t*-map showing activity during successful stop — congruent go in the HRI task. Activations of this masking approach were regarded as significant if they survived $p<.05$ for a for a family wise error (FWE) whole brain correction.

Mutual and distinct neural correlates of response inhibition. Next, the first level analysis results for participant- and condition-specific effects of the HRI task were subjected to full factorial random effects analyses. To identify regions commonly activated during response inhibition, we conducted a conjunction analysis ('conjunction null'; Friston et al., 2005) of 'successful inhibition — go' during interference inhibition, action withholding, and action cancelation in the HRI task. To assess subcomponent specific neural correlates we directly contrasted the three conditions within the HRI task. To assess subcomponent specific activations only within the network of areas demonstrated being active for a particular sub-component, we inclusively masked the respective contrast by the contrast of the particular subcomponent of interest ($p<0.001$). This was necessary, since all contrasts use the same baseline (i.e. congruent go). For instance, when assessing interference inhibition > action withholding, the contrast was masked by the

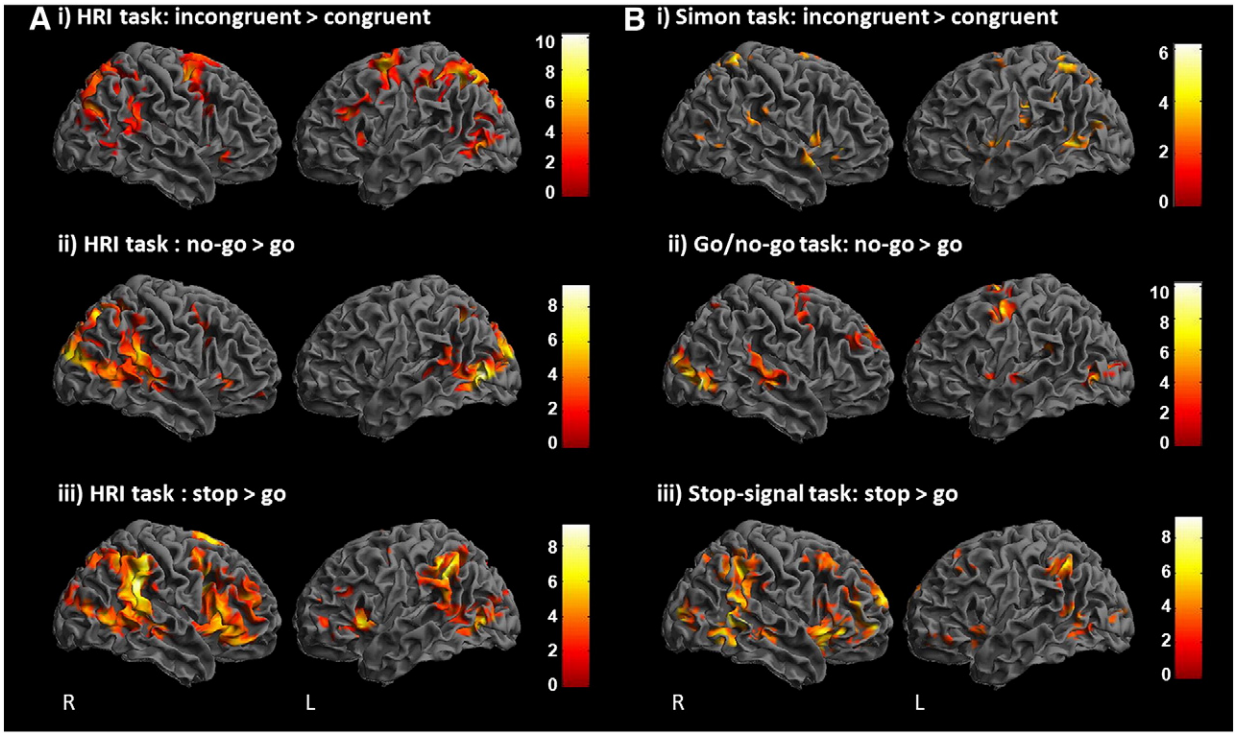

Fig. 3. Activation maps showing significant activation for the contrast 'inhibition–go' for (A) the Hybrid Response Inhibition (HRI) task and (B) the test battery of the separate Simon-, Go/no-go- and Stop-signal tasks: i) interference inhibition, ii) action withholding, and iii) action cancelation (for display purposes: $p<0.001$, k = 10 voxel). Coordinates are reported in MNI-space. The color scale represents *t*-score. R = right, L = left.

Table 2
Brain region associated with successful inhibition in the Hybrid Response Inhibition task.

Region		MNI-coordinates			z-score	*p*	k
		x	*y*	*z*			
Incongruent go > congruent go							
Frontal cortex							
Inferior frontal gyrus (p. orbitalis)	R	48	23	−5	4.36	0.001	140
Inferior frontal gyrus (p. triangularis)	R	42	23	7			
Middle frontal gyrus	R	36	−1	52	5.23	<0.001	1209
Inferior frontal gyrus (p. opercularis)	R	48	11	28			
Superior frontal gyrus	R	24	−1	52			
Precentral gyrus	R	42	−4	43			
SMA/pre-SMA	R	12	5	70			
SMA	L	−3	11	49			
Middle cingulate cortex	R	12	17	34			
Middle frontal gyrus	L	−24	2	55	5.38	<0.001	726
Inferior frontal gyrus (p. triangularis)	L	−42	26	25			
Precentral gyrus (pre-motor cortex)	L	−27	−1	58			
Parietal and occipital cortex							
Superior parietal lobule	L	−24	−61	52	5.99	<0.001	3553
Inferior parietal lobule	L	−39	−37	43			
Precunues	R	12	−58	49			
Precunues	L	−12	−64	49			
Supramarginal gyrus	R	48	−40	31			
Superior occipital gyrus	L	−21	−79	31			
Middle occipital gyrus	R	36	−76	28			
Middle occipital gyrus	L	−27	−76	25			
Subcortical areas							
Caudate	R	15	−19	19	3.45	0.036*	33
Putamen	L	−27	−16	10	3.60	0.023*	119
Thalamus	L	−15	−10	10	4.54	<0.001	395
Thalamus	R	15	−16	16			
No-go > congruent go							
Frontal cortex							
Inferior frontal gyrus (p. triangularis)	R	48	23	−2	4.41	0.004	136
Middle frontal gyrus	R	42	8	37	3.85	0.003	147
Inferior frontal gyrus (p. opercularis)	R	39	5	34			
Precentral gyrus	R	48	8	31			
Parietal, temporal and occipital cortex							
Superior occipital gyrus	R	27	−94	16	5.11	<0.001	1985
Middle occipital gyrus	R	36	−85	19			
Superior parietal lobe	R	27	−67	49			
Superior temporal gyrus	R	63	−34	7			
Middle occipital gyrus	L	−45	−76	4	5.70	<0.001	1104
Superior occipital gyrus	L	−15	−97	16			
Cuneus	L	−12	−88	37			
Fusiform gyrus	L	−39	−58	−11			
Superior parietal lobe	L	−27	−61	46			
Superior temporal gyrus	L	−57	−49	19			
Lingual gyrus	L	−6	−70	1	4.57	0.001	178
Calcarine gyrus	L	−21	−70	13			
Calcarine gyrus	R	24	−67	10			
Stop > congruent go							
Frontal cortex							
Inferior frontal gyrus (pars opercularis)	R	42	8	34	5.81	<0.001	3958
Insula	R	36	20	1			
Middle temporal gyrus	R	54	−61	7			
Inferior parietal lobe	R	39	−49	49			
Supramarginal gyrus	R	48	−40	34			
Inferior frontal gyrus (p. triangularis)	L	−45	20	1	4.95	<0.001	373
Inferior frontal gyrus (p. orbitalis)	L	−33	32	−5			
Insula	L	−33	17	−2			
Middle frontal gyrus	L	−27	44	19	4.19	0.038	76
Inferior frontal gyrus	L	−39	26	25			
SMA/pre-SMA	R	9	14	64	5.09	<0.001	538
Superior frontal gyrus	R	21	8	67			
Superior medial gyrus	L	0	29	49			
Anterior cingulate gyrus	R	6	35	22			
Anterior cingulate gyrus	L	−9	35	22			
Middle cingulate gyrus	R	9	29	31			
Parietal, temporal and occipital cortex							
Inferior parietal lobule	L	−54	−46	43	5.33	<0.001	1049
Supramarginal gyrus	L	−57	−46	34			
Middle occipital gyrus	L	−45	−79	4			
Middle temporal gyrus	L	−42	−58	10			
Subcortical areas							

Table 2 (*continued*)

Region		MNI-coordinates			z-score	*p*	k
		x	*y*	*z*			
Putamen	R	30	14	7	4.38	0.001*	268
Putamen	L	−27	14	4	4.05	0.005*	148
Caudate	R	9	5	10	4.22	0.002*	153
Caudate	L	−12	8	10	3.43	0.032*	129

Local maxima of brain activations during successful inhibition — go in the HRI task in Montreal Neurological Institute (MNI) coordinates with associated *z*-score ($p_{FWE}<.05$, cluster level corrected; * small volume corrected, $p_{FWE}<.05$) and cluster extent in number of voxel (k). Pre-SMA = pre-supplemental motor area. Coordinates of local sub-peaks within a cluster are shown indented; R = right; L = left.

interference inhibition contrast (i.e. incongruent go > congruent go). Since the mask controls for the act of motor responding and, thus, isolates the interference inhibition network itself, regions within the mask showing activity during interference inhibition > action withholding can be concluded as those more strongly involved in interference inhibition. The same logic was applied to the assessment of the other subcomponents. If not stated differently, group results were corrected for multiple comparisons at the cluster level using a height threshold of $p<.05$ FWE correction with an extent threshold of ten contiguous voxels (except for the masking approach, see above). In addition, small volume corrections (SVC) were performed in predefined regions of interest (ROI) following Aron and Poldrack (2006) which were all taken from the automated anatomical labeling atlas (AAL; Tzourio-Mazoyer et al., 2002): right IFC, derived from combination of pars opercularis and pars triangularis, pre-SMA, derived from the SMA region with $y>0$ as well as caudate, putamen and pallidum. Additionally, the right middle frontal gyrus was included as a ROI, as the inferior frontal junction is another central region of the neural inhibitory network (e.g. Chikazoe et al., 2009). Small volume corrected activations were regarded as significant if they survived $p<.05$ for a FWE correction.

Behavioral data analyses. Behavioral data (reaction time (RT) and accuracy) were collected by the Presentation software while subjects performed the tasks in the scanner and analyzed using SPSS®, Version 19. Responses on inhibition trials and no responses on go trials will be referred to as commission errors and omission errors, respectively. Measures of interest were mean reaction time on correct go trials, percentage of commission errors on inhibition trials and omission errors on go trials. The interference effect was computed by subtracting the mean RT of congruent trials from the mean RT of incongruent trials in the HRI task as well as in the Simon task. In the HRI- and the Stop-signal tasks, individual SSDs were varied applying a staircase procedure so as to yield a probability of 50% correct reactions in the stop condition. The Stop-signal reaction time (SSRT) was computed by subtracting the average SSD from median RT for correct reactions in the go condition according to the race model (Logan et al., 1984).

Results

Behavioral performance

Table 1 summarizes behavioral data. Analysis of variance (ANOVA) revealed that in the HRI task, RTs were longer as in the Go/no-go task as were the interference effect and SSRT compared to the separate tasks. This might reflect a higher cognitive load in the HRI task, resulting from the requirements to maintain and apply a more complex set of task rules. However, subjects performed accurately in all tasks with low rates of omission errors in all tasks (<1.5%), and inhibition scores (interference effect, commission error rates and SSRT) differed but were in the same range. Errors during incongruent trials were<2.0% in the HRI task as well as in the Simon task.

Imaging results

Task validation

Individual subcomponent specific activity. To assess the reliability of the newly developed HRI task, we first computed the contrast of 'successful inhibition — go' for each subcomponent separately (Fig. 3A, Table 2). The contrast 'incongruent go — congruent go' revealed activation in bilateral IFC, medial PFC including SMA/pre-SMA, and other pre-motor areas as well as activation in mainly left parietal regions, left putamen, right caudate, and thalamus. The contrast 'no-go — congruent go' revealed activation in right PFC including inferior frontal gyrus, middle frontal gyrus as well as activation in parietal, occipital, and temporal regions. The contrast 'stop — congruent go' revealed activation in bilateral inferior frontal gyri/insulae, a cluster stretching from the anterior cingulate cortex (ACC) to SMA/pre-SMA, bilateral striatal and bilateral parietal regions. Overall, the results were comparable to the activity in the corresponding contrast in the separate tasks (Fig. 3B, Table 3).

Sequential masking approach. To assess whether regions which are significantly activated during interference inhibition, action withholding, and action cancelation in the separate standard tasks are recruited in the newly developed HRI task as well, we conducted a sequential masking procedure (Table 4). For interference inhibition (i.e. the contrast 'incongruent go — congruent go'), activation shared by the classical Simon and the HRI task was revealed in a cluster covering right MFG and pre-motor regions such as superior frontal gyrus, SMA/pre-SMA, and middle cingulate cortex (MCC). Further common activation was found in left pre-motor cortex and left parietal regions. During action withholding (i.e. the contrast 'no-go — go'), common activation was revealed in visual regions. Although prominent clusters were also found in bilateral inferior and superior parietal regions as well as in the right IFC/insula, these did not reach significance. During action cancelation (i.e. the contrast 'stop — go'), common activation was present in a large cluster covering right IFC including pars opercularis, pars triangularis and pars orbitalis, insula, MFG, and pre-motor cortex. Further prominent clusters were found in the left IFC covering pars triangularis, pars opercularis and the insula, as well as in the pre-SMA and in bilateral parietal regions.

Common and component specific neural correlates in the HRI task

Common task activity. Conjunction analysis revealed significant common activation during interference inhibition, action withholding, and action cancelation in the HRI task in a cluster covering right IFC and insula, in the right inferior frontal junction, and in bilateral parietal regions. Small volume correction additionally revealed overlapping activation in the pre-SMA (Fig. 4, Table 5).

Subcomponent specific neural correlates. Contrasting interference inhibition with action withholding revealed activation in bilateral pre-motor areas, the SMA/pre-SMA region, left parietal regions, as well as in the

Table 3
Brain region associated with successful inhibition in the separate Simon- Go/no-go-, and Stop-signal tasks.

Region		MNI-coordinates			z-score	*p*	k
		x	*y*	*z*			
Simon task: incongruent go > congruent go							
Frontal cortex							
Inferior frontal gyrus (p. orbitalis)	R	39	33	−3	4.53	0.003*	166
SMA/pre-SMA	R	15	3	66	3.72	0.037	39
SMA/pre-SMA	L	−3	12	63			
SMA/pre-SMA	L	−6	6	48	4.48	<0.001	287
Anterior cingulate cortex	L	0	30	27			
Middle cingulate cortex	R	9	−18	36			
Middle cingulate cortex	L	−3	−6	39			
Superior medial gyrus	R	9	21	42			
Frontal and temporal cortex							
Superior temporal gyrus	L	−57	−3	3	4.23	<0.001	129
Insula	L	−39	6	9			
Temporal pole	L	−54	12	−3			
Superior temporal gyrus	L	−51	3	12			
Parietal, temporal and occipital cortex							
Middle temporal gyrus	L	−48	−60	3	4.88	<0.001	649
Inferior parietal lobule	L	−27	−48	42			
Precuneus	L	−9	−57	60			
Middle occipital gyrus	L	−24	−66	33			
Superior Parietal lobule	L	−30	−51	63	4.55	0.001	80
Postcentral gyrus	R	30	−48	63	5.05	0.002	69
Temporal Pole	R	54	12	−12	5.05	<0.001	175
Superior temporal gyrus	R	60	−36	18	4.02	0.017	47
Subcortical areas							
Putamen	R	36	−12	−9	3.56	0.042*	13
Pallidum	R	30	−13	−5	3.15	0.022*	7
Go/no-go task: no-go > go							
Frontal cortex							
Middle frontal gyrus	R	36	39	27	4.04	0.049	48
SMA	L	−6	−6	66	5.47	<.001	767
SMA/pre-SMA	R	3	0	63			
SMA/pre-SMA	L	−9	6	54			
Superior frontal gyrus	L	−27	0	66			
Precentral gyrus	L	−45	−3	51			
Middle cingulate gyrus	L	−9	15	36			
Superior frontal gyrus	R	15	48	36	4.74	0.010	73
Middle frontal gyrus	R	24	45	27			
Superior medial gyrus	R	12	57	24			
Precentral gyrus	R	54	6	42	4.11	0.001	113
Middle frontal gyrus	R	45	0	54			
Superior frontal gyrus	R	33	−3	60			
Parietal, temporal and occipital cortex							
Inferior temporal gyrus	R	48	−72	−3	6.31	<0.001	330
Middle occipital gyrus	R	39	−87	3			
Superior occipital gyrus	R	27	−93	12			
Superior temporal gyrus	R	54	−24	−3	5.00	<0.001	239
Superior temporal gyrus	R	66	−33	21			
Middle occipital gyrus	L	−51	−75	3	5.05	<0.001	170
Superior occipital gyrus	L	−15	−96	9			
Calcarine gyrus	L	−6	96	9			
Subcortical areas							
Caudate	R	18	−6	21	3.67	0.022*	206
Caudate	L	−9	0	15	3.51	0.035*	216
Putamen	R	27	6	6	4.06	0.001	120
Putamen	L	−24	9	9	4.60	0.004	87
Stop-signal task: stop > go							
Frontal cortex							
Insula	R	30	18	−12	5.42	<0.001	562
Inferior frontal gyrus (p. orbitalis)	R	45	27	−6			
Inferior frontal gyrus (p. opercularis)	R	54	15	3			
Middle frontal gyrus	R	36	54	0			
Middle orbital gyrus	R	36	51	−12			
Insula	L	−39	15	−6	4.64	0.020	57
Middle frontal gyrus	R	39	24	48	3.94	0.002	92
Precentral gyrus	R	51	6	45			
Superior frontal gyrus	R	18	60	21	4.93	<0.001	174
Parietal cortex							
Inferior parietal lobule	L	−51	−54	48	4.75	<0.001	139
Supramarginal gyrus	L	−57	−45	27			
Temporal and occipital cortex							
Middle temporal gyrus	L	−57	−60	9	4.48	<0.001	126

Table 3 (*continued*)

Region		MNI-coordinates			z-score	*p*	k
		x	*y*	*z*			
Inferior temporal gyrus	L	−57	−60	−6			
Inferior occipital gyrus	L	−45	−72	−3			
Fusiform gyrus	L	−42	−57	−12			
Fusiform gyrus	R	30	−54	−15	5.52	<0.001	1235
Inferior temporal gyrus	R	48	−57	−12			
Middle temporal gyrus	R	63	−42	3			
Superior temporal gyrus	R	60	−48	21			
Supramarginal gyrus	R	48	−42	42			
Subcortical areas							
Caudate	L	−12	6	15	3.42	0.049*	27
Putamen	R	30	15	−3	3.68	65	

Local maxima of brain activations during successful inhibition − go in the Simon-, Go/no-go-, and Stop-signal tasks in Montreal Neurological Institute (MNI) coordinates with associated *z*-score (p_{FWE}<.05, cluster level corrected; * small volume corrected, p_{FWE}<.05) and cluster extent in number of voxel (k). Pre-SMA = pre-supplemental motor area. Coordinates of local sub-peaks within a cluster are shown indented; R = right; L = left.

right caudate. Interference inhibition as compared to action cancelation was associated with increased activation in left pre-/sensorimotor areas and left parietal regions. Contrasting action withholding to action cancelation revealed no significantly activated regions. When contrasting action withholding with interference inhibition, increased activation was present in mainly visual areas. The contrast of action cancelation minus interference inhibition resulted in activation in bilateral IFC/insulae, right striatum, and visual areas. Comparing action cancelation with action withholding resulted in increased activation again in bilateral IFC/insulae, pre-SMA, right striatum, and left inferior parietal lobule (Fig. 5, Table 6).

Discussion

This study sought to systematically assess functional specialization of the neural inhibitory network during distinguishable subcomponents of response inhibition, i.e. interference inhibition, action withholding, and action cancelation. Therefore, we developed a novel paradigm, the Hybrid Response Inhibition (HRI) task, allowing us to assess these subcomponents and their underlying neural subprocesses within the same individuals and the same task using identical stimulus material. The results provide evidence for functional distinctive activation patterns of those subcomponents along with evidence for an overlapping network of shared activation. Common activation was found in key regions of the inhibitory network, specifically in the right posterior IFC and the pre-SMA as well as bilateral parietal regions. This finding underlines our assumption that interference inhibition, action withholding, and action cancelation all represent subcomponents of response inhibition and it is well in line with previous studies (Levy and Wagner, 2011; McNab et al., 2008; Nee et al., 2007; Rubia et al., 2001; Swick et al., 2011).

Moreover, we were particularly interested in subcomponent-specific activation patterns. Action cancelation compared to interference inhibition as well as action withholding revealed stronger activation in bilateral posterior IFC/insulae and right striatum. Region of interest analysis hints at progressive activity in these fronto-striatal regions from interference inhibition via action withholding to action cancelation (see Fig. 5). This is in line with findings of a meta-analysis by Levy and Wagner (2011) who reported increased activation in the posterior IFC with increasing stopping demands as this is the case for action cancelation compared to interference inhibition or action withholding. Our finding further suggests that inhibiting an already initiated reaction might rely more strongly on the (indirect) fronto-striatal pathway. This is analogous to Jahfari et al. (2011) who recently reported effective connectivity analyses of a combined Simon/Stop-signal task. They suggest that the indirect (fronto-striatal–pallidal) and hyperdirect (fronto-subthalamic) pathways complementally implement action cancelation. Although we did not find direct evidence for engagement of the hyperdirect pathway (STN activation was subthreshold), we cannot rule out that it was differentially engaged in these processes as well.

Interference inhibition compared to action withholding and action cancelation revealed activation mainly in pre-motor and parietal regions. Pre-motor regions have been found to be more strongly activated during interference inhibition induced by stimulus–response conflict (Simon task) as opposed to stimulus–stimulus conflict (e.g. Stroop task; Egner et al., 2007; Liu et al., 2004; Wendelken et al., 2009). Especially anterior parietal regions such as the left supramarginal gyrus are associated with motor attention and particularly with disengaging and redirecting such attentional processes (Rushworth et al., 2001a, 2001b; Schiff et al., 2011). Predominantly left dorsal premotor regions are associated with motor response selection (Chouinard, 2006; Cisek and Kalaska, 2005; Laird et al., 2005). This suggests that interference inhibition might be closely related to motor attention and action selection processes and may implement inhibition via pre-motor regions/cortico-cortical connections to a greater extent than action withholding and action cancelation. Thus, two neural networks could be involved during interference inhibition: first, response-related interference inhibition could engage a fronto-parietal–pre-motor network during response selection. In addition, the indirect fronto-striatal loop with activation of rIFC and caudate is needed while response inhibition is finally implemented during interference inhibition.

Contrasting action withholding to action cancelation or interference inhibition revealed either no activation differences or increased activation mainly in visual association areas, respectively (aside from non-significant trends in frontal and motor regions). This finding was somewhat unexpected, as previous studies contrasting action withholding to action cancelation reported increased activation in the middle frontal gyrus, pre-SMA, and parietal regions when comparing independent tasks (Rubia et al., 2001; Swick et al., 2011). Our seemingly deviant result might be explained by action withholdings' putative nested placement between interference inhibition and action cancelation in the process of response control. Converging evidence suggests that action withholding and action cancelation might interfere at different time points within the action generation or action inhibition process to implement response inhibition (Dalley et al., 2011; Eagle et al., 2008; Nee et al., 2007; Schachar et al., 2007; Sebastian et al., 2012). In the Go/no-go task, the no-go signal is presented at the same time point as the go signal. In the Stop-signal task, the stop-signal is presented at some delay after the go signal. This seemingly subtle difference has been associated with distinct activation patterns (McNab et al., 2008; Rubia et al., 2001; Swick et al., 2011). Considering the present findings in concert with the existing evidence, we would suggest extending the framework to at least three subcomponents of response inhibition, putatively interfering in a sequential fashion in the action inhibition sequence (Fig. 1A). Within this framework, interference inhibition would resemble an early subcomponent. From a neuropsychological point of view, interference inhibition requires

Table 4
Task validation.

Region		MNI-coordinates			z-score	*p*	k
		x	*y*	*z*			
Interference inhibition							
Frontal cortex							
Middle frontal gyrus	R	33	−1	52	5.06	0.010	631
Superior frontal gyrus	R	18	−4	61			
SMA/pre-SMA	R	12	5	70			
SMA/pre-SMA	L	−3	11	49			
Middle cingulate gyrus	R	12	17	34			
Pre-central gyrus	L	−27	−1	58	5.34	0.002	375
Superior frontal gyrus	L	−21	−7	73			
Postcentral gyrus	L	−45	10	52			
Parietal and occipital cortex							
Superior parietal lobule	L	−24	−61	52	5.99	<0.001	2489
Inferior parietal lobule	L	−39	−37	43			
Precuneus	R	12	−58	49			
Precuneus	L	−12	−64	49			
Supramarginal gyrus	R	48	−40	31			
Middle occipital gyrus	R	36	−76	28			
Middle occipital gyrus	L	−27	−85	34			
Superior occipital gyrus	L	−21	−79	31			
Action withholding							
Occipital, parietal and temporal cortex							
Superior occipital gyrus	R	27	−94	16	5.11	0.008	1070
Middle occipital gyrus	R	36	−85	19			
Superior parietal lobule	R	27	−67	49			
Superior temporal gyrus	R	63	−34	7			
Middle occipital gyrus	L	−45	−76	4	5.70	<0.001	239
Superior occipital gyrus	L	−15	−97	16			
Cuneus	L	−9	−94	13			
Action cancelation							
Frontal cortex							
Inferior frontal gyrus (p. opercularis)	R	42	8	34	5.81	<0.001	1081
Inferior frontal gyrus (p. triangularis)	R	51	20	7			
Inferior frontal gyrus (p. orbitalis)	R	45	35	−11			
Insula	R	36	20	1			
Middle frontal gyrus	R	36	44	19			
Precentral gyrus	R	36	5	49			
Insula	L	−33	17	−2	4.86	0.033	172
Inferior frontal gyrus (p. triangularis)	L	−48	17	1			
Inferior frontal gyrus (p. opercularis)	L	−57	14	10			
Pre-SMA	R	9	17	61	4.99	0.013	197
Anterior cingulate cortex	R	6	35	22			
Superior medial gyrus	L	0	29	40			
Parietal and temporal cortex							
Supramarginal gyrus	R	48	−40	34	5.60	<0.001	1476
Inferior parietal lobule	R	39	−49	49			
Middle temporal gyrus	R	54	−61	7			
Superior temporal gyrus	R	63	−37	22			
Inferior parietal lobule	L	−54	−46	43	5.33	0.001	702
Supramarginal gyrus	L	−57	−46	34			
Middle temporal gyrus	L	−54	−49	22			
Middle occipital gyrus	L	−45	−79	4			
Fusiform gyrus	L	−39	−52	−11			

Local maxima of brain activations commonly activated during successful inhibition — go in the HRI task and the separate tasks as revealed by a sequential masking procedure (cf. methods section Group analysis) in Montreal Neurological Institute (MNI) coordinates with associated *z*-score (p_{FWE}<.05) and cluster extent in number of voxel (k). Interference inhibition: incongruent — congruent; action withholding: no-go — go; action cancelation: stop — go. Coordinates of local sub-peaks within a cluster are shown indented; R = right; L = left.

inhibition of response tendencies which are involuntary activated by task irrelevant stimulus features (Simon and Berbaum, 1990) and which are thought to arise before response initiation. Our imaging results further indicate that interference inhibition activates regions related to response selection processes more strongly than the other presently considered subcomponents. This corroborates its role as an early subcomponent of response inhibition. Action cancelation, however, would be a late subcomponent as it assesses – in contrast to the other subcomponents – inhibition of an ongoing response. Action withholding would be positioned in between as it comprises aspects of action selection in addition to inhibitory aspects (Eagle et al., 2008; Mostofsky and Simmonds, 2008; Rubia et al., 2001). This is further underlined by a meta-analysis by Nee et al. (2007) who report overlapping activation in Go/No-go and Stop-Signal tasks in regions implied in response execution, whereas activation in Stroop, Flanker, and Go/No-go tasks overlapped in regions thought to mediate response selection. That, in turn, fits very well with the present imaging findings: Since action withholding was associated with activation in key regions of the inhibitory network as revealed by the conjunction analysis on the one hand, but did not differ in such regions when compared to interference inhibition or action cancelation on the other hand, it supports the idea of action withholding as an intermediate subcomponent of response inhibition within a sequence of interference inhibition, action withholding, and action cancelation. This assumption is further

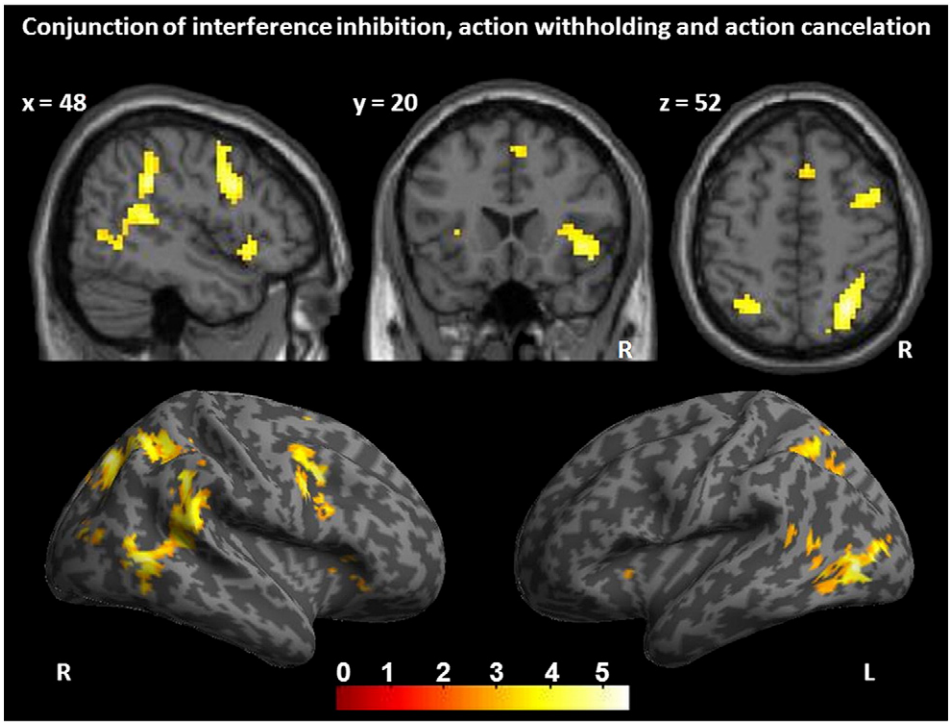

Fig. 4. Activation maps showing common activation for successful inhibition ('inhibition minus go') during interference inhibition, action withholding and action cancelation in the Hybrid Response Inhibition task (for display purposes: $p<0.001$, k = 10 voxel). Coordinates are reported in MNI-space. The color scale represents *t*-score. R = right, L = left.

underlined by quantitative progression in activity during action cancelation > action withholding > interference inhibition in fronto-striatal regions, whereas the opposite pattern is present in the left inferior parietal cortex (see Fig. 5).

Whether the right IFC or the pre-SMA primarily implements inhibitory control is still heavily debated. There is broad evidence in the literature that the rIFC, especially the posterior part of the rIFC, plays a pivotal role in response inhibition (Aron, 2011; Aron and Poldrack, 2006; Chambers et al., 2006, 2007; Chevrier et al., 2007; Chikazoe et al., 2009; Garavan et al., 1999; Rubia et al., 2003; Swann et al., 2012). Yet, it might also be involved in attentional processing of a stop-signal (Boehler et al., 2011; Dodds et al., 2011; Hampshire et al., 2010; Sharp et al., 2010). Some authors have, thus, argued that the pre-SMA rather than the rIFC might be critical for response inhibition (Chao et al., 2009; Duann et al., 2009; Floden and Stuss, 2006; Li et al., 2006; Sharp et al., 2010). The differential activation patterns in the IFC and pre-SMA in our study point towards a primary role of the IFC for the implementation of stopping, whereas the pre-SMA is more strongly involved in response selection. As outlined

Table 5
Brain regions mutually associated with different aspects of response inhibition.

Region		MNI-coordinates			z-score	*p*	k
		x	*y*	*z*			
Frontal cortex							
Inferior frontal cortex/insula	R	42	20	−5	4.05	0.042	82
Inferior frontal gyrus (p. opercularis)	R	39	5	34	5.44	0.001	196
Middle frontal gyrus	R	45	5	55			
Pre-SMA	R	6	20	52	3.51	0.039*	180
Parietal, temporal and occipital cortex							
Angular gyrus	R	30	−61	49	4.92	<0.001	904
Inferior parietal lobule	R	36	−49	40			
Supramarginal gyrus	R	48	−40	31			
Middle temporal gyrus	R	57	−58	1			
Superior temporal gyrus	R	60	−43	19			
Superior occipital gyrus	R	27	−73	46			
Superior parietal lobe	L	−27	−61	49	4.06	0.003	164
Precuneus	L	−15	−64	34			
Middle occipital gyrus	L	−21	−61	34			
Superior occipital gyrus	L	−9	−82	43			
Occipital and temporal cortex							
Middle occipital gyrus	L	−45	−76	4	5.49	<0.001	226
Inferior temporal gyrus	L	−45	−64	−5			
Middle temporal gyrus	L	−42	−55	10			

Local maxima of brain activations commonly activated during successful inhibition − go in the HRI task as revealed by conjunction across all subcomponents in Montreal Neurological Institute (MNI) coordinates with associated *z*-score ($p_{FWE}<.05$, cluster level corrected; * small volume corrected, $p_{FWE}<.05$) and cluster extent in number of voxel (k). Coordinates of local sub-peaks within a cluster are shown indented; R = right; L = left.

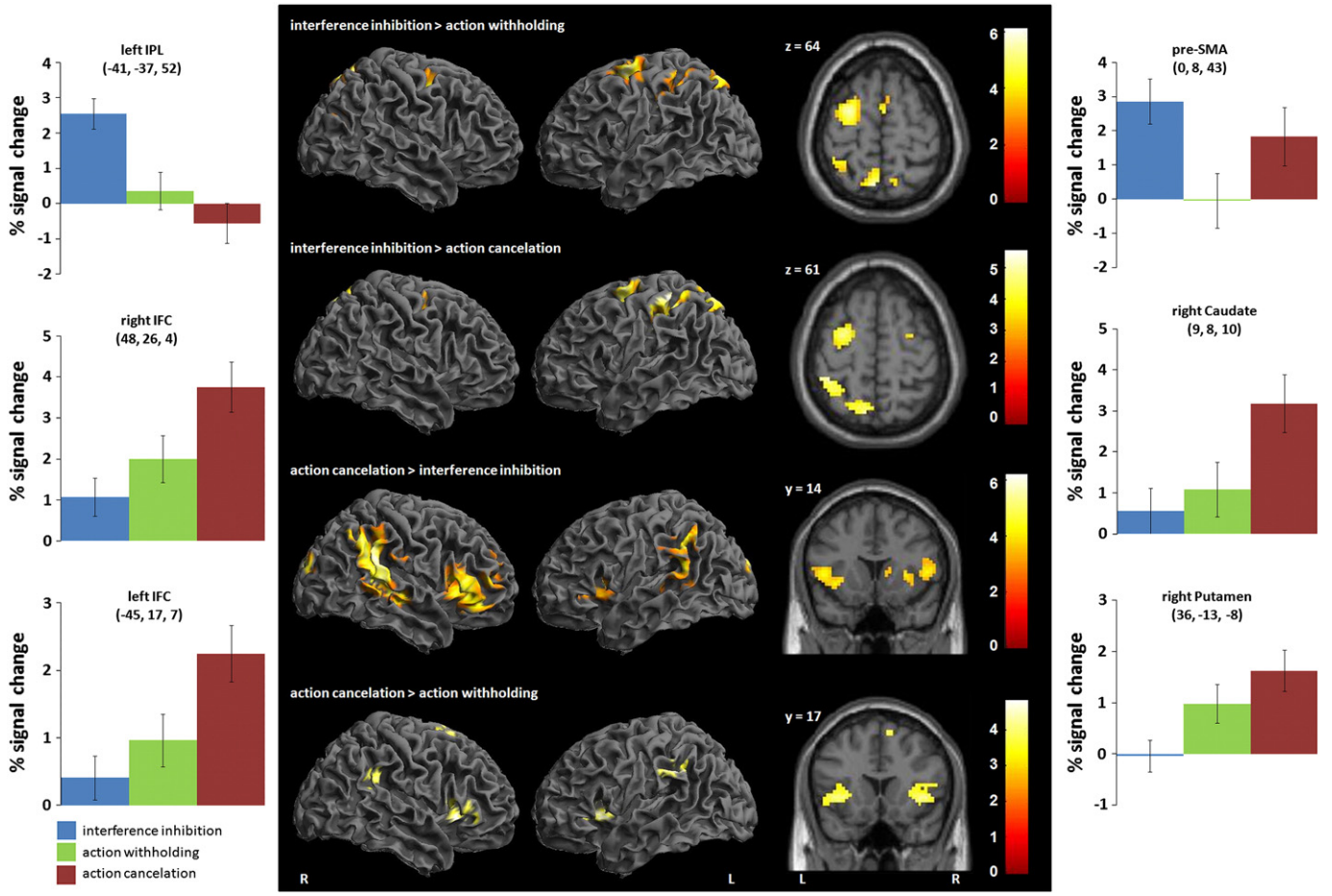

Fig. 5. Subcomponent specific neural correlates are revealed by contrasting the subcomponents of the Hybrid response inhibition controlled for the motor response. Interference inhibition corresponds to 'incongruent go − congruent go'; action withholding corresponds to 'no-go − congruent go'; action cancelation corresponds to 'stop − congruent go' (for display purposes: $p<0.001$, k = 10 voxel). Contrast estimates are shown for regions of interest: IFC = inferior frontal cortex; IPL = inferior parietal lobule; pre-SMA = pre-supplemental motor area; error bars indicate standard error of the mean. Coordinates are reported in MNI-space. The color scale represents *t*-score. R = right, L = left.

above, increased IFC activation was present during action cancelation (more than during interference inhibition or action withholding) corroborating earlier results (Levy and Wagner, 2011; Swick et al., 2011). Of note, this activation was located in the posterior part of the IFC. Recent findings suggest a functional dissociation of the posterior IFC and the inferior frontal junction for inhibitory and attentional processes, respectively (Chikazoe et al., 2009; Levy and Wagner, 2011; Verbruggen et al., 2010). Jahfari et al. (2011) also provide indirect support for a predominant role of the rIFC in implementing inhibitory control: higher connection strengths between rIFC and caudate were associated with more efficient action cancelation whereas higher connection strengths between pre-SMA and caudate were associated with poorer inhibition. This is in agreement with findings from transcranial magnetic stimulation studies reporting inhibitory and fascilitatory effects of IFC and pre-SMA on M1, respectively (Mars et al., 2009; Neubert et al., 2010). Further support stems from a recent study employing transcranial direct current stimulation over the rIFC resulting in improved action cancelation (Jacobson et al., 2012). Taken together with our results, these findings convergently suggest that the rIFC is engaged predominantly in inhibitory processes.

The specific role of the pre-SMA in inhibition is less clear, as it has been associated with different functions such as conflict solving (Forstmann et al., 2008), action selection (as one form of inhibition) (Mostofsky and Simmonds, 2008) or in task set configuration (Neubert et al., 2010; Rushworth et al., 2004; Swann et al., 2012). In the present study, increased pre-SMA activation was seen during interference inhibition and action cancelation more than during action withholding. Interference inhibition and action cancelation might differ from action withholding, in that the former two conditions involve a spatial response selection (left or right button press) and a movement initiation. This is reflected in relatively longer RTs in the separate Simon- and Stop-signal tasks than in the Go/no-go task. However during action withholding, subjects select between responding and withholding a response. Although these processes compete (which obviously reflects another mode of response selection as well), go-processes are not necessarily involved during action withholding. Mostofsky and Simmonds (2008) have argued that response selection is akin to response inhibition inasmuch as the appropriate "response" in response inhibition is to inhibit an inappropriate response and that both processes are neurally indiscernible. However, our data suggest stronger pre-SMA activation when the appropriate reaction involves down-stream movement execution (e.g. initiating and retracting the movement in case of a stop trial or actually performing a button press in case of an incongruent trial) than when selecting to withhold a movement.

Another line of literature suggests that activity in the dorsal medial wall including the dorsal ACC and the SMA/pre-SMA region varies with time on task, i.e. response duration even after controlling for effects of incongruency (Carp et al., 2010; Grinband et al., 2011). Thus, increased pre-SMA activity during action cancelation and interference inhibition as compared to action withholding might also be associated with increased RT during those subcomponents which might well fit with the interpretation that this region is critically involved in response

Table 6
Functional specification of subcomponents of response inhibition.

Region		MNI-coordinates			z-score	*p*	k
		x	*y*	*z*			
Interference inhibition > action withholding							
Frontal cortex							
Middle frontal gyrus	R	27	−24	52	3.94	0.022*	54
SMA/pre-SMA	L	0	8	43	3.56	0.033*	260
Superior frontal gyrus	R	24	−13	49	4.55	0.021	101
Superior frontal gyrus	L	−21	2	58	5.37	<0.001	351
Precunues	L	−39	−13	55			
Parietal cortex							
Inferior parietal lobule	L	−42	−37	52	4.39	0.001	215
Superior parietal lobule	L	−33	−46	64			
Postcentral gyrus	L	−36	−43	61			
Precuneus	L	−6	−64	61	5.11	<0.001	316
Precunues	R	9	−61	55			
Subcortical areas							
Caudate	R	18	−19	19	3.27	0.046*	7
Interference inhibition > action cancelation							
Frontal cortex							
Superior frontal gyrus	L	−27	−4	64	4.46	0.001	128
Parietal cortex							
Inferior parietal lobule	L	−42	−37	52	4.98	<0.001	262
Superior parietal lobule	L	−33	−49	61			
Postcentral gyrus	L	−36	−34	43			
Precuneus	L	−12	−73	55	4.39	0.004	148
Action withholding > interference inhibition							
Temporal and occipital cortex							
Superior temporal sulcus	R	48	−28	1	4.44	<0.001	232
Middle temporal gyurs	R	63	−37	4			
Superior occipital gyrus	R	18	−97	19	7.02	0.001	184
Cuneus	L	−9	−97	16	5.69	0.014	111
Superior occipital gyrus	L	−21	−97	19			
Action cancelation > interference inhibition							
Frontal cortex							
Inferior frontal gyrus (p. triangularis)	R	48	26	4	5.28	<0.001	609
Inferior frontal gyrus (p. orbitalis)	R	42	38	−8			
Middle frontal gyrus	R	45	44	10			
Insula	R	39	23	−5			
Inferior frontal gyrus (p. triangularis)	L	−45	17	7	4.14	0.001	187
Inferior frontal gyrus (p. opercularis)	L	−48	14	4			
Insula	L	−36	14	−5			
Parietal and temporal cortex							
Inferior parietal lobule	R	63	−40	25	5.43	< 0.001	927
Middle temporal gyrus	R	48	−40	7			
Superior temporal gyrus	R	45	−28	1			
Angular gyrus	R	54	−58	46			
Putamen	R	36	−13	−8			
Superior temporal gyrus	L	−60	−46	19	5.39	< 0.001	270
Inferior parietal lobule	L	−51	−58	49			
Middle temporal gyrus	L	−51	−52	7			
Subcortical areas							
Caudate	R	9	8	10	3.55	0.020*	53
Action cancelation > action withholding							
Frontal cortex							
Insula	R	36	23	−5	4.45	0.001	195
Inferior frontal gyrus (p. triangularis)	R	39	23	7			
Inferior frontal gyrus (p. opercularis)	R	45	17	10			
Insula	L	−36	14	1	3.94	0.003	160
Inferior frontal gyrus (p. opercularis)	L	−48	11	1			
Pre-SMA	R	12	8	58	3.73	0.019*	281
Parietal cortex							
Supramarginal gyrus	L	−63	−37	34	3.96	0.039	84
Subcortical areas							
Putamen	R	30	14	7	3.28	0.044*	50
Caudate	R	18	−4	16	3.30	0.042*	53

Local maxima of brain activations specifically activated during successful inhibition − go in one of the subcomponents of the HRI task in Montreal Neurological Institute (MNI) coordinates with associated *z*-score (p_{FWE}<.05, cluster level corrected; * small volume corrected, p_{FWE}<.05) and cluster extent in number of voxel (k). Interference inhibition: incongruent − congruent; action withholding: no-go − go; action cancelation: stop − go. Pre-SMA = pre-supplemental motor area. Coordinates of local sub-peaks within a cluster are shown indented; R = right; L = left.

selection. Yet, inhibition in the presence of competing behavioral alternatives seems inseparable from action selection processes. Thus, the pre-SMA might fulfill a double function.

To the best of our knowledge, this is the first study to assess interference inhibition, action withholding, and action cancelation within one paradigm using fMRI. Activation patterns related to all subcomponents tapped by the HRI task were comparable to activation as captured by separate standard tasks in the present as well as in previous studies (e.g. Aron and Poldrack, 2006; Garavan et al., 1999; Kerns, 2006; McNab et al., 2008; Rubia et al., 2001). Reliability of the activation patterns was further confirmed by an inclusive masking approach, which revealed common activation especially during interference inhibition and action cancelation in key regions of the inhibitory network. Although activation patterns for action withholding in the HRI- and the Go/no-go tasks were comparable, mutual activation in inhibitory key regions failed to reach significance in the masking procedure. Both tasks reveal activity in prefrontal regions including the middle frontal gyrus and pre-motor areas. However, while pre-SMA activity was only present in the separate Go/no-go task, activity in parietal regions was associated with action withholding in the HRI task only. Differences between experiments in first level modeling and stimulus material might account for reduced overlap in these regions during action withholding. First, interstimulus intervals in the separate Go/no-go task were shorter as compared to the HRI task and were therefore used as an active baseline. Further, verbal stimulus material was used in the separate Go/no-go task whereas arrows were employed in the HRI task. This involves further differences between the tasks: in the separate Go/no-go task, only a single response is required (i.e. right button press) whereas in the HRI task the subject is required to choose between two alternatives (i.e. left or right button press which might also account for activation in parietal regions associated with spatial processing). In turn, in the separate Go/no-go task the response can be prepared in advance to stimulus onset which is not the case in the HRI task. This might account for pre-SMA activity which was not revealed during action withholding in the HRI task. Both tasks further differ in the salience of the no-go stimulus with presumably increased perceptive salience in the HRI task. Altogether, these differences might not only account for little significant overlap of activation patterns in both tasks, but also for differences in behavioral measures like the commission error rate and reaction times alike.

In sum, we have developed a paradigm which reliably captures three subcomponents of response inhibition, i.e. interference inhibition, action withholding and action cancelation. While engaging a shared neural network, they might constitute subsequent subcomponents intervening in the action generation process at different points in time to implement response inhibition. Earlier subcomponents like interference inhibition might more strongly engage fronto-parietal–pre-motor circuits whereas the later action cancelation subcomponent relies more strongly on the (indirect) prefrontal–striatal pathway. The HRI task disentangles subprocesses of response inhibition and their neural correlates, a feature that is highly demanded in the literature. We, thus, provide a valid tool to assess imminent questions about differences in cognitive components and neural processes of response inhibition. In addition, it might help to further our understanding of impairments in different disorders sharing impulsivity as a core symptom.

Acknowledgments

This work was supported by the Federal Ministry of Education and Research grant 01GW0730 (AV, CS, CK, KL and OT). We would like to thank the Freiburg Brain Imaging Center, especially Volkmar Glauche, for continuous support, Arian Mobascher for helpful comments on the manuscript, and Birthe Gerdes, Carlos Baldermann, Julian Geißhardt, Lena Schmüser, and Tanja Schmitt for assistance in data collection.

References

Aron, A.R., 2011. From reactive to proactive and selective control: developing a richer model for stopping inappropriate responses. Biol. Psychiatry 69, e55–e68.
Aron, A.R., Poldrack, R.A., 2006. Cortical and subcortical contributions to stop signal response inhibition: role of the subthalamic nucleus. J. Neurosci. 26, 2424–2433.
Band, G.P., van Boxtel, G.J., 1999. Inhibitory motor control in stop paradigms: review and reinterpretation of neural mechanisms. Acta Psychol. 101, 179–211.
Barkley, R.A., 1997. Behavioral inhibition, sustained attention, and executive functions: constructing a unifying theory of ADHD. Psychol. Bull. 65–94.
Boehler, C., Appelbaum, L., Krebs, R., Hopf, J., Woldorff, M., 2010. Pinning down response inhibition in the brain — conjunction analyses of the Stop-signal task. Neuroimage 52, 1621–1632.
Boehler, C.N., Appelbaum, L.G., Krebs, R.M., Chen, L.-C., Woldorff, M.G., Wenderoth, N., 2011. The role of stimulus salience and attentional capture across the neural hierarchy in a Stop-signal task. PLoS One 6, e26386.
Carp, J., Kim, K., Taylor, S.F., Fitzgerald, K.D., Weissman, D.H., 2010. Conditional differences in mean reaction time explain effects of response congruency, but not accuracy, on posterior medial frontal cortex activity. Front. Hum. Neurosci. 4, 231.
Chao, H.H.A., Luo, X., Chang, J.L.K., Li, C.-S.R., 2009. Activation of the pre-supplementary motor area but not inferior prefrontal cortex in association with short stop signal reaction time — an intra-subject analysis. BMC Neurosci. 10, 75.
Chambers, C.D., Bellgrove, M.A., Stokes, M.G., Henderson, T.R., Garavan, H., Robertson, I.H., Morris, A.P., Mattingley, J.B., 2006. Executive "Brake Failure" following deactivation of human frontal lobe. J. Cogn. Neurosci. 18, 444–455.
Chambers, C.D., Bellgrove, M.A., Gould, I.C., English, T., Garavan, H., McNaught, E., Kamke, M., Mattingley, J.B., 2007. Dissociable Mechanisms of Cognitive Control in Prefrontal and Premotor Cortex. J. Neurophysiol. 98, 3638–3647.
Chevrier, A.D., Noseworthy, M.D., Schachar, R., 2007. Dissociation of response inhibition and performance monitoring in the stop signal task using event-related fMRI. Hum. Brain Mapp. 28, 1347–1358.
Chikazoe, J., 2010. Localizing performance of go/no-go tasks to prefrontal cortical subregions. Curr. Opin. Psychiatry 23, 267–272.
Chikazoe, J., Jimura, K., Asari, T., Yamashita, K.-I., Morimoto, H., Hirose, S., Miyashita, Y., Konishi, S., 2009. Functional Dissociation in right inferior frontal cortex during performance of Go/no-go task. Cereb. Cortex 19, 146–152.
Chouinard, P.A., 2006. The primary motor and premotor areas of the human cerebral cortex. Neuroscientist 12, 143–152.
Cisek, P., Kalaska, J.F., 2005. Neural correlates of reaching decisions in dorsal premotor cortex: specification of multiple direction choices and final selection of action. Neuron 45, 801–814.
Dalley, J.W., Everitt, B.J., Robbins, T.W., 2011. Impulsivity, compulsivity, and top–down cognitive control. Neuron 69, 680–694.
Dodds, C.M., Morein-Zamir, S., Robbins, T.W., 2011. Dissociating inhibition, attention, and response control in the frontoparietal network using functional magnetic resonance imaging. Cereb. Cortex 21, 1155–1165.
Duann, J.-R., Ide, J.S., Luo, X., Li, C.-S.R., 2009. Functional connectivity delineates distinct roles of the inferior frontal cortex and presupplementary motor area in stop signal inhibition. J. Neurosci. 29, 10171–10179.
Eagle, D.M., Bari, A., Robbins, T.W., 2008. The neuropsychopharmacology of action inhibition: cross-species translation of the stop-signal and go/no-go tasks. Psychopharmacology 199, 439–456.
Egner, T., Delano, M., Hirsch, J., 2007. Separate conflict-specific cognitive control mechanisms in the human brain. Neuroimage 35, 940–948.
Evenden, J.L., 1999. Varieties of impulsivity. Psychopharmacology 146, 348–361.
Floden, D., Stuss, D.T., 2006. Inhibitory control is slowed in patients with right superior medial frontal damage. J. Cogn. Neurosci. 18, 1843–1849.
Forstmann, B.U., Jahfari, S., Scholte, H.S., Wolfensteller, U., van den Wildenberg, W.P.M., Ridderinkhof, K.R., 2008. Function and structure of the right inferior frontal cortex predict individual differences in response inhibition: a model-based approach. J. Neurosci. 28, 9790–9796.
Friston, K.J., Penny, W.D., Glaser, D.E., 2005. Conjunction revisited. Neuroimage 25, 661–667.
Frühholz, S., Godde, B., Finke, M., Herrmann, M., 2011. Spatio-temporal brain dynamics in a combined stimulus–stimulus and stimulus–response conflict task. Neuroimage 54, 622–634.
Garavan, H., Ross, T.J., Stein, E.A., 1999. Right hemispheric dominance of inhibitory control: an event-related functional MRI study. Proc. Natl. Acad. Sci. 96, 8301–8306.
Grinband, J., Savitskaya, J., Wager, T.D., Teichert, T., Ferrera, V.P., Hirsch, J., 2011. The dorsal medial frontal cortex is sensitive to time on task, not response conflict or error likelihood. Neuroimage 57, 303–311.
Hampshire, A., Chamberlain, S.R., Monti, M.M., Duncan, J., Owen, A.M., 2010. The role of the right inferior frontal gyrus: inhibition and attentional control. Neuroimage 50, 1313–1319.
Jacobson, L., Ezra, A., Berger, U., Lavidor, M., 2012. Modulating oscillatory brain activity correlates of behavioral inhibition using transcranial direct current stimulation. Clin. Neurophysiol. 123, 979–984.
Jahfari, S., Waldorp, L., van den Wildenberg, W.P.M., Scholte, H.S., Ridderinkhof, K.R., Forstmann, B.U., 2011. Effective connectivity reveals important roles for both the hyperdirect (fronto-subthalamic) and the indirect (fronto-striatal–pallidal) fronto-basal ganglia pathways during response inhibition. J. Neurosci. 31, 6891–6899.
Kerns, J.G., 2006. Anterior cingulate and prefrontal cortex activity in an FMRI study of trial-to-trial adjustments on the Simon task. Neuroimage 33, 399–405.
Klöppel, S., Vongerichten, A., van Eimeren, T., Frackowiak, R.S.J., Siebner, H.R., 2007. Can left-handedness be switched? Insights from an early switch of handwriting. J. Neurosci. 27, 7847–7853.

Laird, A.R., Fox, P.M., Price, C.J., Glahn, D.C., Uecker, A.M., Lancaster, J.L., Turkeltaub, P.E., Kochunov, P., Fox, P.T., 2005. ALE meta-analysis: controlling the false discovery rate and performing statistical contrasts. Hum. Brain Mapp. 25, 155–164.
Levy, B.J., Wagner, A.D., 2011. Cognitive control and right ventrolateral prefrontal cortex: reflexive reorienting, motor inhibition, and action updating. Ann. N. Y. Acad. Sci. 1224, 40–62.
Li, C.S., Huang, C., Constable, R.T., Sinha, R., 2006. Imaging response inhibition in a stop-signal task: neural correlates independent of signal monitoring and post-response processing. J. Neurosci. 26, 186–192.
Liu, X., Banich, M., Jacobson, B., Tanabe, J., 2004. Common and distinct neural substrates of attentional control in an integrated Simon and spatial Stroop task as assessed by event-related fMRI. Neuroimage 22, 1097–1106.
Logan, G.D., Cowan, W.B., Davis, K.A., 1984. On the ability to inhibit responses in simple and choice reaction time tasks: a model and a method. J. Exp. Psychol. Hum. Percept. Perform. 276–291.
Mars, R.B., Klein, M.C., Neubert, F.-X., Olivier, E., Buch, E.R., Boorman, E.D., Rushworth, M.F.S., 2009. Short-latency influence of medial frontal cortex on primary motor cortex during action selection under conflict. J. Neurosci. 29, 6926–6931.
McNab, F., Leroux, G., Strand, F., Thorell, L., Bergman, S., Klingberg, T., 2008. Common and unique components of inhibition and working memory: an fMRI, within-subjects investigation. Neuropsychologia 46, 2668–2682.
Miyake, A., Friedman, N.P., Emerson, M.J., Witzki, A.H., Howerter, A., Wager, T.D., 2000. The unity and diversity of executive functions and their contributions to complex "frontal lobe" tasks: a latent variable analysis. Cognit. Psychol. 41, 49–100.
Mostofsky, S.H., Simmonds, D.J., 2008. Response inhibition and response selection: two sides of the same coin. J. Cogn. Neurosci. 20, 751–761.
Nee, D.E., Wager, T.D., Jonides, J., 2007. Interference resolution: insights from a meta-analysis of neuroimaging tasks. Cogn. Affect. Behav. Neurosci. 7, 1–17.
Neubert, F.-X., Mars, R.B., Buch, E.R., Olivier, E., Rushworth, M.F.S., 2010. Cortical and subcortical interactions during action reprogramming and their related white matter pathways. Proc. Natl. Acad. Sci. 107, 13240–13245.
Nigg, J.T., 2000. On inhibition/disinhibition in developmental psychopathology: views from cognitive and personality psychology and a working inhibition taxonomy. Psychol. Bull. 126, 220–246.
Oldfield, R.C., 1971. The assessment and analysis of handedness: the Edinburgh inventory. Neuropsychologia 9, 97–113.
Rubia, K., Russell, T., Overmeyer, S., Brammer, M., Bullmore, E., Sharma, T., Simmons, A., Williams, S., Giampietro, V., Andrew, C., 2001. Mapping motor inhibition: conjunctive brain activations across different versions of Go/no-go and stop tasks. Neuroimage 13, 250–261.
Rubia, K., Smith, A.B., Brammer, M.J., Taylor, E., 2003. Right inferior prefrontal cortex mediates response inhibition while mesial prefrontal cortex is responsible for error detection. Neuroimage 20, 351–358.
Rushworth, M.F., Krams, M., Passingham, R.E., 2001a. The attentional role of the left parietal cortex: the distinct lateralization and localization of motor attention in the human brain. J. Cogn. Neurosci. 13, 698–710.
Rushworth, M.F., Ellison, A., Walsh, V., 2001b. Complementary localization and lateralization of orienting and motor attention. Nat. Neurosci. 4, 656–661.
Rushworth, M.F.S., Walton, M.E., Kennerley, S.W., Bannerman, D.M., 2004. Action sets and decisions in the medial frontal cortex. Trends Cogn. Sci. 8, 410–417.
Schachar, R., Logan, G.D., Robaey, P., Chen, S., Ickowicz, A., Barr, C., 2007. Restraint and cancellation: multiple inhibition deficits in attention deficit hyperactivity disorder. J. Abnorm. Child Psychol. 35, 229–238.
Schiff, S., Bardi, L., Basso, D., Mapelli, D., 2011. Timing spatial conflict within the parietal cortex: a TMS study. J. Cogn. Neurosci. 23, 3998–4007.
Sebastian, A., Gerdes, B., Feige, B., Klöppel, S., Lange, T., Philipsen, A., van Tebartz Elst, L., Lieb, K., Tüscher, O., 2012. Neural correlates of interference inhibition, action withholding and action cancelation in adult ADHD. Psychiatry Res. 202, 132–141.
Sharp, D.J., Bonnelle, V., de Boissezon, X., Beckmann, C.F., James, S.G., Patel, M.C., Mehta, M.A., 2010. Distinct frontal systems for response inhibition, attentional capture, and error processing. Proc. Natl. Acad. Sci. 107, 6106–6111.
Simon, J.R., Berbaum, K., 1990. Effect of conflicting cues on information processing: the 'Stroop effect' vs. the 'Simon effect'. Acta Psychol. 73, 159–170.
Swann, N.C., Cai, W., Conner, C.R., Pieters, T.A., Claffey, M.P., George, J.S., Aron, A.R., Tandon, N., 2012. Roles for the pre-supplementary motor area and the right inferior frontal gyrus in stopping action: Electrophysiological responses and functional and structural connectivity. Neuroimage 59, 2860–2870.
Swick, D., Ashley, V., Turken, A.U., 2011. Are the neural correlates of stopping and not going identical? Quantitative meta-analysis of two response inhibition tasks. Neuroimage 56, 1655–1656.
Thesen, S., Heid, O., Mueller, E., Schad, L.R., 2000. Prospective acquisition correction for head motion with image-based tracking for real-time fMRI. Magn. Reson. Med. 44, 457–465.
Tzourio-Mazoyer, N., Landeau, B., Papathanassiou, D., Crivello, F., Etard, O., Delcroix, N., Mazoyer, B., Joliot, M., 2002. Automated anatomical labeling of activations in SPM using a macroscopic anatomical parcellation of the MNI MRI single-subject brain. Neuroimage 15, 273–289.
Verbruggen, F., Logan, G.D., 2008. Response inhibition in the stop-signal paradigm. Trends Cogn. Sci. 12, 418–424.
Verbruggen, F., Liefooghe, B., Notebaert, W., Vandierendonck, A., 2005. Effects of stimulus–stimulus compatibility and stimulus–response compatibility on response inhibition. Acta Psychol. 120, 307–326.
Verbruggen, F., Aron, A.R., Stevens, M.A., Chambers, C.D., 2010. Theta burst stimulation dissociates attention and action updating in human inferior frontal cortex. Proc. Natl. Acad. Sci. 107, 13966–13971.
Wendelken, C., Ditterich, J., Bunge, S.A., Carter, C.S., 2009. Stimulus and response conflict processing during perceptual decision making. Cogn. Affect. Behav. Neurosci. 9, 434–447.
Wittchen, H., Zaudig, M., Frydrich, T., 1997. Strukturiertes Klinisches Interview für DSM-IV (SKID-I und SKID-II). Hogrefe, Göttingen.
Zaitsev, M., Hennig, J., Speck, O., 2004. Point spread function mapping with parallel imaging techniques and high acceleration factors: fast, robust, and flexible method for echo-planar imaging distortion correction. Magn. Reson. Med. 52, 1156–1166.
Zheng, D., Oka, T., Bokura, H., Yamaguchi, S., 2008. The key locus of common response inhibition network for no-go and stop signals. J. Cogn. Neurosci. 20, 1434–1442.